



# Assessing the Collection Efficiency of Natural Cloud Particles Impacting the Nevzorov Total Water Content Probe

George A. Isaac<sup>\*</sup>, Alexei V. Korolev, J. Walter Strapp, Stewart G. Cober  
*Cloud Physics and Severe Weather Research Section, Environment Canada,  
Toronto, Ontario, M3H 5T4, Canada*

Faisal S. Boudala  
*Department of Physics and Atmospheric Science, Dalhousie University  
Halifax, Nova Scotia, B3H 3J5, Canada*

Dave Marcotte  
*Flight Research Laboratory, National Research Council of Canada  
Ottawa, Ontario, K1A 0R6, Canada*

and

Vincent L. Reich  
*InDyne Inc at NASA Glenn Research Center, Cleveland, Ohio, 44135*

The Nevzorov Total Water Content Probe has been used extensively for characterizing the cloud water content (ice and liquid) in clouds where airframe icing and engine related problems might occur. Because of recent work done in the ice simulating wind tunnels, where a significant fraction of ice particles were observed to be ejected from the sensor instead of captured and evaporated, it is suspected that the Nevzorov Total Water probe and other similar hot-wire sensors are providing underestimates of ice water content and possibly even liquid water content in the presence of large drops. In-flight tests were performed in December 2004 where natural ice particles (dendritic ice crystals and aggregates) and water drops were photographed impacting a specially mounted Nevzorov probe installed on the NRC Convair-580. A high speed camera captured small fragments of ice particles and water drops being swept out of the collecting cone of the total water sensor after impact. It appears that the Nevzorov probe is detecting a decreasing fraction of the mass of individual particles (solid and liquid) with increasing particle size, although this effect could not be quantified with the available data. It should be emphasized that even when ice crystal shattering was occurring with subsequent loss of mass, the Nevzorov probe was still detecting a fraction of the ice. One of the interesting observations was the apparent difference in the visual impression of natural particle impacts during the flight tests versus simulated ice impacts in the wind tunnel tests. Particles did not “bounce” out of the sensor as they appeared to in the tunnel experiments, but appeared to shatter into small fragments, some of which would be ejected from the sensor in a complicated manner. This difference is postulated to be due to the higher density of simulated ice particles in the tunnel. The current tests documented impacts with natural cloud ice particles that would be classified as “fragile” and usually with a low density. The results suggest that both wind tunnel and in-situ tests are needed to fully describe probe performance in ice particle environments.

---

<sup>\*</sup> Corresponding Author: George A. Isaac, Senior Scientist, Cloud Physics and Severe Weather Research Section, Environment Canada, 4905 Dufferin Street, Toronto, Ontario, M3H5T4, Canada. E-Mail: george.isaac@ec.gc.ca

## I. Introduction

Measuring or characterizing the liquid and ice water contents of clouds is quite important in order to assess airframe or engine icing severity. The Nevzorov Total Water Content (TWC) probe (Korolev et al., 1998) has been used for many years on some research aircraft to measure the liquid and ice water contents of clouds. Calibration of the efficiency of the TWC sensor in ice particle conditions is elusive due to the lack of any absolute reference for comparison. Korolev et al. (1998) showed that the TWC sensor had an efficiency close to unity for very small frozen water droplets of 20  $\mu\text{m}$  MVD. However, some recent papers describing instrument performance testing in ice particle conditions at the Cox and Co. Icing Wind Tunnel (Al-Khalil et al. 2003) have shown that the probe may underestimate ice water content (IWC) (e.g. Emery et al. 2004; Strapp et al. 2005) due to particle bouncing and pooling and subsequent shedding of water from the sensor before complete evaporation. IWC measurements from different hot wire geometries were found to vary by more than a factor of two (Strapp et al. 2005). Because of these potential errors, it was decided to run tests in natural clouds, where it is known that the turbulence, particle trajectories, and particularly the ice particle properties would be different. The ice particles produced in the wind tunnel studies above are produced by shaving ice blocks, and likely have a higher density and less fragile structure than vapour-grown ice crystals. A series of tests were conducted using the National Research Council (NRC) Convair-580 between 17 and 20 December 2004 using a total of 16.7 flight hours. The particles striking the Total Water Sensor of the Nevzorov Probe were imaged using a Phantom v5 high speed camera. The results of these tests are reported below.

## II. Equipment Description

The NRC Convair-580 was instrumented with its normal complement of cloud microphysical probes as summarized in Table 1. The equipment onboard the aircraft for aircraft icing studies has been previously described by Isaac et al. (2001 a,b) and most recently by Isaac et al. (2005) for the AIRS II campaign.

Parameter	Instrument
Temperature	Rosemount (x2), Reverse Flow,
Dewpoint	EG&G Cambridge, LI-COR
Pressure (True Airspeed Barometric Alt.) Accelerations Angle of Attack Attitude and Rates Winds and Gusts	Paroscientific Series 1000 Litton 90-100 IRS Rosemount 858,
Navigation	IRS Litton 90-100 GPS Novatel (x2), Trimble
Liquid/Total Water	PMS King LWC (x2) Nevzorov TWC/LWC (wing and fuselage mounts) SEA J-W TWC
Aerosol Droplets Hydrometeors	PMS PCASP 0.1-3 $\mu\text{m}$ PMS FSSP 100 3-45 $\mu\text{m}$ PMS 2DC Mono 25-800 $\mu\text{m}$ PMS 2D-2C Mono 25-800 $\mu\text{m}$ PMS 2DC Gray 15-960 $\mu\text{m}$ PMS 2DP Mono 200-6400 DMT CIP (12-768 $\mu\text{m}$ ) SPEC Cloud Particle Imager
Remote Sensing	35 GHz (3 cm) Aircraft Weather Radar Ka-Band Cloud Radar Nevzorov Extinction Probe
Icing	Rosemount 871FA Vibro-meter Icing Detector

Table 1: Equipment as installed on the NRC Convair-580 for the Nevzorov Probe Test Flights

The Nevzorov probe tested has been described by Korolev et al. (1998). Figure 1 shows a schematic of the probe itself and how it functions. The probe has a liquid water content (LWC) sensor and a total water content (TWC) sensor. The TWC sensor consists of a cone that faces into the airstream guided by a vane that orients the cone directly into the airflow. The LWC and TWC sensors consist of close single layer windings of enamel-covered nickel wire. For the TWC probe, the collector winding is cemented to the hollow cone at the end of a plastic (textolite) cylinder, and the reference sensor is wound within a shallow groove cut into the same cylinder (Fig. 1b). For the LWC probe, both collector and reference sensors are wound on solid copper rods and cemented to the opposite edges of a flat textolite plate. The diameter of the conical sample area of the TWC collector is 8 mm, and the cone angle is  $120^\circ$ , making its depth approximately 3.5 mm. The cylindrical LWC collector measures 1.8 mm in diameter by 16 mm in length.

The phase discrimination capability of the TWC and LWC collectors results from the difference in the expected behavior of liquid and solid particles impacting with their surfaces. Small liquid droplets, after collision with LWC or TWC collector sensors, should be flattened into a thin surface film and should completely evaporate (Figs. 1a, b). Ice particles should tend to remain inside the conical hollow of the TWC collector (Fig. 1b) until they melt and evaporate. However, ice particles are expected to instantly break away from the convex surface of the LWC collector (Fig. 1a) with negligible heat expended relative to that for complete ice evaporation. In reality ice particles are detected by the LWC collector as shown by Korolev et al. (1998), Cober et al. (2001) and Strapp et al. (1999). This implies that some ice particles or portions of ice particles can be melted and evaporated after colliding with the sensor and before they can be bounced or swept away. For this test, Nevzorov measurements were made with two probes: one mounted on an underwing pylon with other LWC and TWC sensors, and a second identical probe mounted on the top of the fuselage. The underwing pylon is the standard mounting location for this probe and it has been shown to work quite adequately in this location (Cober et al., 2001; Boudala et al., 2002) for small droplet and drizzle measurements, through comparison with other "hot wire" probes and through integration of the size distribution of the PMS FSSP and OAP probes. Figure 2 shows a comparison of an integrated spectra TWC, obtained using PMS FSSP and OAP probes in all liquid clouds, with the Nevzorov TWC, as a function of median volume diameter. These data were obtained using the Nevzorov underwing probe on flights previous to the ones reported here. When the drops are small, with median volume diameter (MVD) less than  $150\text{ }\mu\text{m}$ , the integrated spectrum TWC and the Nevzorov TWC agree quite well. However, as the drops get larger, especially at MVD greater than  $300\text{ }\mu\text{m}$ , the Nevzorov is reading up to 40% less than the integrated spectrum. So, it suggests that the Nevzorov TWC sensor is underestimating at larger drop sizes, although this conclusion is dependent on the unestablished accuracy of the FSSP and OAP spectrum TWC measurements in these all liquid cases. Comparisons of Nevzorov-derived ice mass in glaciated conditions to mass calculations from the PMS OAP probes have also shown very high correlation, although the accuracy of OAP-derived ice mass is insufficient to make any final conclusions about overall Nevzorov accuracy in ice particle conditions.

A special pylon was constructed and mounted on the top fuselage of the Convair-580 to allow a Nevzorov Total Water Sensor to be photographed with a high speed camera (see Fig. 3). The longitudinal location of the probe was at 55% aft of the nose, just aft of the wing trailing edge. The distance from the aircraft skin to the probe sensor was 38.4 cm, and the distance from the skin to the illumination source was 49.5 cm. It was known that there would exist a shadow zone for large particles on top of the fuselage (see later discussion) so several other mounting locations were considered. A location on the side of the fuselage forward of the props was rejected because ice being shed from the probe might interact with the props. A nose or wing mounted probe would not have allowed the necessary access for the operator to the camera. So the location selected, by necessity, was a compromise.

The camera was manufactured by Vision Research, Inc. It is a Phantom V5.0 model with a  $1024 \times 1024$  CMOS imager. Almost all data were captured at  $256 \times 128$  pixels, with a camera exposure time of  $10\text{ }\mu\text{s}$ . The actual exposure was much shorter, because it was controlled by the "pulse length" of an LED flasher. The LED flasher was a custom built piece, consisting of a red LED that pulsed at the Phantom frame rate. The Phantom camera sent a TTL pulse to the LED flasher and fired one flash per frame. The length of that pulse was controlled via a dial on the back of the LED flasher. The LED incorporated a collimated lens that created parallel light waves focused on the lens of the Phantom camera. Diffusion (on the back side of the LED lens) was necessary to soften the light. The Nevzorov was placed 40 cm from the Phantom lens, and approximately 10 cm from the LED lens. Alignment and rigidity of these systems was critical, and performed as expected. The frame rate used for the tests was either 6,000 or 22,000 per second. For 22,000 frames per second, 3 seconds of data could be collected on each "Run" with a downtime of 5 minutes while the data was being stored on disk. The sensor was viewed directly from the side, and there was an ambiguity in determining whether particles with trajectories towards the TWC sensor actually entered the sensor, or passed behind or in front of the sensor. This was one of the primary reasons that mass-loss results

from this experiment could not be quantified. This problem might be solved in the future with an angled view, and/or with special lighting.

### III. Description of Field Tests

The aircraft had one flight on each day between 17 to 20 December for a total of 16.7 flight hours. A total of 40 camera runs were done in-flight resulting in approximately 80 Gb of image data.

The mounting location on the upper fuselage did cause problems. King (1984, 1985 and 1986) and Twohy and Rogers (1993) have discussed problems associated with mounting probes on aircraft. For a top-of-fuselage mount, a shadow zone can exist for some distance above the aircraft skin for particles of a certain size, because the intermediate-sized particles are forced to cross the streamlines as they go over the nose and windscreen. Some calculations were done for the Convair-580 configuration following the approach of King (1984). Figure 4 shows that for a distance about 40 cm from the fuselage skin, a shadow zone exists for particles larger than about 120  $\mu\text{m}$ , although very large particles with sufficient inertia would cross all streamlines and still be sampled (e.g. Twohy and Rogers, 1993). Although this shadowing problem was known during the design of the pylon, the sensing area could not be extended further into the airstream because of cost and structural limitations. It should be noted that the trajectory analysis of King excludes shear effects which in this case might be significant. During the actual field tests, it was discovered that the theoretical predictions of the shadow zone were qualitatively correct. The test pylon gave TWC values similar to the wing Nevzorov probe when the Convair-580 flew in small droplet clouds. However, when large particles were observed, the Nevzorov TWC was only detecting a fraction of the mass, whether they were solid or liquid. Consequently, porpoise maneuvers (or pitch oscillations) and flight with flaps down were conducted to try and minimize the effect of the shadow zone and therefore increase the collection rate of the probe. The results reported in this paper come from periods when the aircraft was operated with flaps down (23 degrees). In normal level flight, the aircraft attitude is about +2 degrees and with flaps at 23 degrees, this changes to -1.5 degrees or a nose down configuration. For these flap down periods, the percentage of mass detected, especially for larger sizes, was increased substantially. However, relatively high IWC ( $> 0.1 \text{ g m}^{-3}$ ) values in large sizes were needed, with the aircraft operating with flaps down, in order to get a sufficient number of good images given the sampling statistics of the camera system.

The short flight on 17 December was mainly used for tests to improve the light conditions and the quality of the videos. During the flight on 18 December, glaciated clouds were encountered and good images were obtained. On 19 December, the aircraft was flown to a precipitating system in a successful attempt to acquire data in liquid clouds with large drops. On 20 December, the objective was to acquire more data in glaciated clouds, but the unexpected presence of supercooled drizzle made operations difficult since the camera pylon was not de-iced. Suitable ice clouds were not found on this day.

### IV. Results

Some impacts of ice crystals with the Nevzorov TWC sensor on 18 December are documented in Figs. 5 and 6. These images were obtained from Run 6 of that day while the aircraft was flying at 5,600 ft at a temperature of approximately  $-10.5^\circ\text{C}$ . The ice particles were mainly either dendrites or aggregates of dendrites (Fig. 7). In Fig. 5, an ice particle approximately 1 mm in size impacted the cone of the Nevzorov TWC sensor. Subsequently, a large number of small particles, easily several hundred, can be seen to eject out of the cone towards the bottom of the frame. Some of these fragments actually traveled several mm forward of the cone against the airflow. Many fragments also traveled sideways (down in the photo) away from the cone by perhaps 4 mm. It is difficult to see these small fragments on the images presented in this paper. Capturing frames from the videos for presentation is a difficult process. The small particle debris is quite clear in the original videos.

Figure 6 shows an ice particle, perhaps 1.5 mm in size, striking the edge of the cone and producing a large number of small fragments. Again, these fragments seem to go forward and sideways from the cone by a substantial distance.

Figure 8 shows the time history of the Nevzorov wing mounted probe and the top of fuselage probe TWC for a period bracketing Run 6 on 18 December which was done near 21:18 UTC. The PMS 2DC and 2DP integrated spectra ice water contents were also calculated following the technique of Korolev and Strapp (2002) and compared with the Nevzorov wing mounted probe TWC. The comparison of the integrations with the wing Nevzorov are quite reasonable, with the integration tracking up and down with the Nevzorov TWC, and the absolute magnitude being similar. However, as Korolev and Strapp indicated, the agreement in TWC may just represent a fortuitous selection of diameter to mass relationship for the integrated value. The Nevzorov fuselage mounted probe detected

approximately 10% of the TWC of the Nevzorov probe in the standard mounting location. However, when flying in clouds with small droplets, the TWC for the two Nevzorov probes were within 10% of each other.

Some impacts of large drops with the Nevzorov probe on 19 December are documented in Figs. 9 and 10. These photos were from Run 8 of that day while the aircraft was flying at 4,600 ft with the temperature of +4.5°C. Images from the PMS 2DC Gray probe from this run are shown in Fig. 11. In Fig. 9, a drop of about 750  $\mu\text{m}$  in size appears to hit near the centre of the cone. Many splash droplets are observed first coming from one side and then the other of the cone. Once again, these fragments go several mm forward into the airstream, and also move sideways away from the cone.

Figure 10 shows a drop about 500  $\mu\text{m}$  in size impacting with the side of the sensor cone. Figure 9c was taken exactly at the time of impact and the middle of the drop appears to strike the edge. The resulting splash pattern is quite interesting, creating an arc of small droplets some of which also go forward from the cone into the airstream.

Figure 12 shows the time history of the Nevzorov wing mounted probe and the top of fuselage probe TWC for a period bracketing Run 8 on 19 December which was done near 16:45 UTC. During this period, the pitch angle of the aircraft is also plotted and it is clearly at values less than -1 degree for most of the time. The PMS 2DC and 2DP integrated spectra ice water contents were also calculated assuming spherical particles and compared with the Nevzorov wing mounted probe TWC. Most of the mass was in the 2DC size range. The comparison of the 2DC integration with the wing Nevzorov is also quite reasonable, with the integration tracking up and down with the Nevzorov TWC, and the absolute magnitude being similar. The Nevzorov fuselage mounted probe detected approximately 84% of the TWC of the Nevzorov probe in the standard mounting location for this large drop case.

It should be mentioned that the airflow at the location of the tested Nevzorov sensor head was not parallel to the TWC sensor. It is approximately 5 degrees off in yaw, as can be seen from the particle trajectories on the video. There is also a strong shear. The evidence of this can be seen in Figs. 9a and b where the shape of the drop is not spherical and it appears to change from the first image (Fig. 9a) to the second one (Fig. 9b). The shear and non-parallel airflow create additional forces which might affect particles being swept from the TWC sensor cone.

One of the interesting and unique aspects of these images, especially those of the ice particle impacts, is the complicated detail that can be observed when a fragile ice crystal impacts the TWC sensor. For example, in some cases it appears that the crystal can impact one end of the cone, travel down into the bottom of the cone, and then back up the other side and eject as a partial debris trail. Comparison of these images to past images taken at the Cox and Co. icing wind tunnel, where ice particle conditions were simulated using shaved ice, reveals some significant differences. The wind tunnel data are predictably different in visual impression, due to the fact that much of the data were taken in constant illumination rather than flashed illumination as in the case of the airborne data. In the case of most of the wind tunnel data, individual particles appear as streaks due to their exposure time. In the case of the airborne data, particle motion is frozen and they can be observed more or less in their natural form. Their movement is shown by translation in subsequent frames. In this regard, it would be very difficult to see particle breakup and subsequent debris in the wind tunnel data, although it could be possible had the camera been set up in the same manner as the airborne tests. However, it is possible to subjectively conclude that there is more of an appearance of particle bouncing in the case of the wind tunnel data, a behaviour attributed to the fact that the wind tunnel shaved ice particle are probably significantly more dense and less fragile than those sampled in the airborne studies. Regardless, a TWC sensor must be able to sample both fragile and dense compact particles, since both likely occur in nature, these tests illustrate that value of airborne in-situ instrument testing.

## V. Conclusions and Recommendations

A number of conclusions can be made from these tests:

- 1) These tests with high speed imagery provided some unique insights into the physics of cloud/precipitation particle impacts with airborne probes.
- 2) The Nevzorov probe appears to be detecting only a fraction the mass of large (>500  $\mu\text{m}$ ) ice particles impacting with the TWC sensor. That fraction cannot be quantified using the results of these tests but it suggests that further work is required. The results are qualitatively consistent with past studies in wind tunnels suggesting underestimation of IWC by the Nevzorov and other hot-wire TWC devices (Strapp et al., 2005).
- 3) Although the high speed camera was operated in a different mode between the wind tunnel and airborne tests, it appears that the ice particle impacts observed in the airborne studies were substantially different than those observed in the wind tunnel (Emery et al., 2004; Strapp et al., 2005). No obvious “bouncing” was observed. Particles appeared to breakup up into many particles, with some of the particle debris ejected from the sensor. However, the ice particles observed were mainly

dendritic or aggregates of small crystals, and were quite fragile. The Cox tunnel particles did not tend to reach sizes larger than about 500  $\mu\text{m}$ , and were probably of higher density.

4) Some of the ice particle impacts resulted in a large number (100s) of small ice fragments being produced. This is similar to what Korolev and Isaac (2005) inferred for some snow particle impacts with cloud microphysical imaging probes.

5) The splashing of some large drops ( $>500 \mu\text{m}$ ) in size also suggests that the Nevzorov probe will underestimate liquid water mass of drizzle and rain but the amount of underestimation was not quantified.

6) The tendency of the small fragments produced (both liquid and ice) to move forward into the airstream and sideways away from the sensor has interesting implications for cloud microphysical measurements made by probes which have protruding leading edges such as sampling tubes and forward-facing arms. Some anomalous readings might result if fragments resulting from impacts entered into the sampling areas.

These tests also lead to a number of possible recommendations:

1) For future in-flight tests, careful consideration should be given to proper mounting of the camera and probes so as to avoid the shadowing and alignment effects observed during these studies. A belly or wing mount might be more suitable. It is highly desirable to mount the camera and LED where the operator has access to it inside the fuselage. Mounting the camera outside the fuselage or in a restricted area is not desired, but might be possible in some circumstances.

2) It was not possible to unambiguously determine which particles were actually impacting the sensor, thus making it impossible to quantify what fraction of impacts resulted in particle debris ejected from the sensor. This might be solved with an angled view, and/or with special lighting.

3) More tests are required to determine the collection efficiency of the Nevzorov TWC sensor and other hot wire TWC devices for large ice and water particles under a wide range of conditions. It is suggested that these tests could be conducted in wind tunnels to determine performance in conditions of dense compact ice particles under relatively controlled conditions, but should also be performed in natural clouds that can contain “fragile” and low-density particles. Both high and low density particles may occur in natural clouds.

4) When testing probes or aircraft sections for operation in ice particles (snow or ice clouds), it would be prudent to assess whether it is necessary to conduct tests with particles that resemble naturally occurring ice particles. This might require in-flight tests or tests done during natural snow events.

## Acknowledgments

Besides the contributions of their own organizations, the authors would like to acknowledge the financial support of Transport Canada, the FAA, and the Icing Research Branch of NASA Glenn.

## References

- Al-Khalil, K., E. Irani, and D. Miller, “Mixed-phase icing simulation and testing at the Cox Icing Wind Tunnel” *41st AIAA Aerospace Sciences Meeting And Exhibit*, Jan. 2003, AIAA-2003-0903
- Boudala, F.S., G.A. Isaac, Q. Fu, and S.G. Cober, 2002: Parameterization of effective ice particle sizes for high latitude clouds. *Inter. J. Climatol.*, **22**, 1267-1284.
- Cober, S.G. and G.A. Isaac, 2006: Estimating maximum aircraft icing environments using a large data base of in-situ observations. *44th AIAA Aerospace Sci. Meeting and Exhibit*, Reno Nevada, January 2006. AIAA-2006-0266.
- Cober, S.G., G.A. Isaac, A.V. Korolev and J.W. Strapp, 2001: Assessing cloud-phase conditions. *J. Appl. Meteor.*, **40**, 1967-1983.
- Cober, S.G., G.A. Isaac and J.W. Strapp, 2001: Characterizations of aircraft icing environments that include supercooled large drops. *J. Appl. Meteor.*, 1984-2002.
- Emery, E., Miller, D., Plaskon, S., Strapp, J.W., And Lilie, L.E., “Ice particle impact on cloud water content Instrumentation,” *42nd AIAA Aerospace Sciences Meeting And Exhibit*, Jan. 2004, AIAA-2004-0731.
- Isaac, G.A., S.G. Cober, J.W. Strapp, D. Hudak, T.P. Ratvasky, D.L. Marcotte, and F. Fabry 2001a: Preliminary results from the Alliance Icing Research Study (AIRS). *AIAA 39th Aerospace Sci. Meeting and Exhibit*, Reno Nevada, 8-11 January 2001, AIAA 2001-0393.
- Isaac, G.A., S.G. Cober, J.W. Strapp, A.V. Korolev, A. Tremblay, and D.L. Marcotte, 2001b: Recent Canadian research on aircraft in-flight icing. *Canadian Aeronautics and Space Journal*, **47**, 213-221.

- Isaac, G.A., J.K. Ayers, M. Bailey, L. Bissonnette, B.C. Bernstein, S.G. Cober, N. Driedger, W.F.J. Evans, F. Fabry, A. Glazer, I. Gultepe, J. Hallett, D. Hudak, A.V. Korolev, D. Marcotte, P. Minnis, J. Murray, L. Nguyen, T.P. Ratvasky, A. Reehorst, J. Reid, P. Rodriguez, T. Schneider, B.E. Sheppard, J.W. Strapp, and M. Wolde, 2005: First results from the Alliance Icing Research Study II. *43<sup>rd</sup> AIAA Aerospace Sci. Meeting and Exhibit*, Reno Nevada, 11-13 January 2005, AIAA 2005-0252.
- King, W.D., 1984: Air Flow and Particle Trajectories around Aircraft Fuselages. I: Theory. *J. Atmos. Oceanic Tech.*, 1, 5–13.
- King, W.D., 1985: Air flow and particle trajectories around aircraft fuselages. Part III: Extensions to particles of arbitrary shape. *J. Atmos. Oceanic Tech.*, 4, 539–547.
- King, W.D., 1986: Air flow and particle trajectories around aircraft fuselages. IV: Orientation of ice crystals. *J. Atmos. Oceanic Tech.*, 3, 433–439.
- Korolev, A.V., and J.W. Strapp, 2002: Accuracy of measurements of cloud ice water content by the Nevzorov probe. *40<sup>th</sup> AIAA Aerospace Sci. Meeting and Exhibit*, Reno Nevada, 14-17 January 2002, AIAA 2002-0679.
- Korolev, A.V., and G.A. Isaac, 2005: Shattering during sampling by OAPs and HVPS. Part 1: Snow particles. *J. Atmos. Oceanic Tech.*, 22, 528-542.
- Korolev, A.V., J.W. Strapp, G.A. Isaac, and A. Nevzorov, 1998: The Nevzorov airborne hot wire LWC/TWC probe: Principles of operation and performance characteristics. *J. Atmos. and Oceanic Tech.*, 15, 1495-1510.
- Strapp, J.W., P. Chow, M. Maltby, A.D. Bezer, A.V. Korolev, I. Stromberg, and J. Hallett, 1999: Cloud microphysical measurements in thunderstorm outflow regions during Allied/BAE 1997 flight trials. *27<sup>th</sup> AIAA Aerospace Sci. Meeting and Exhibit*, Reno Nevada, 11-14 January 1999, AIAA 99-0498.
- Strapp, J.W., L. E. Lilie, E. Emery and D. Miller, 2005: Preliminary comparison of ice water content as measured by hot wire instruments of varying configuration,” *43<sup>rd</sup> AIAA Aerospace Sciences Meeting, Reno, Nevada*, 11-13 January 2005, AIAA-2005-0860.
- Twohy, Cynthia H. and Diana Rogers. 1993: Airflow and water-drop trajectories at instrument sampling points around the Beechcraft King Air and Lockheed Electra. *J. Atmos. Oceanic Tech.*, 4, 566–578.

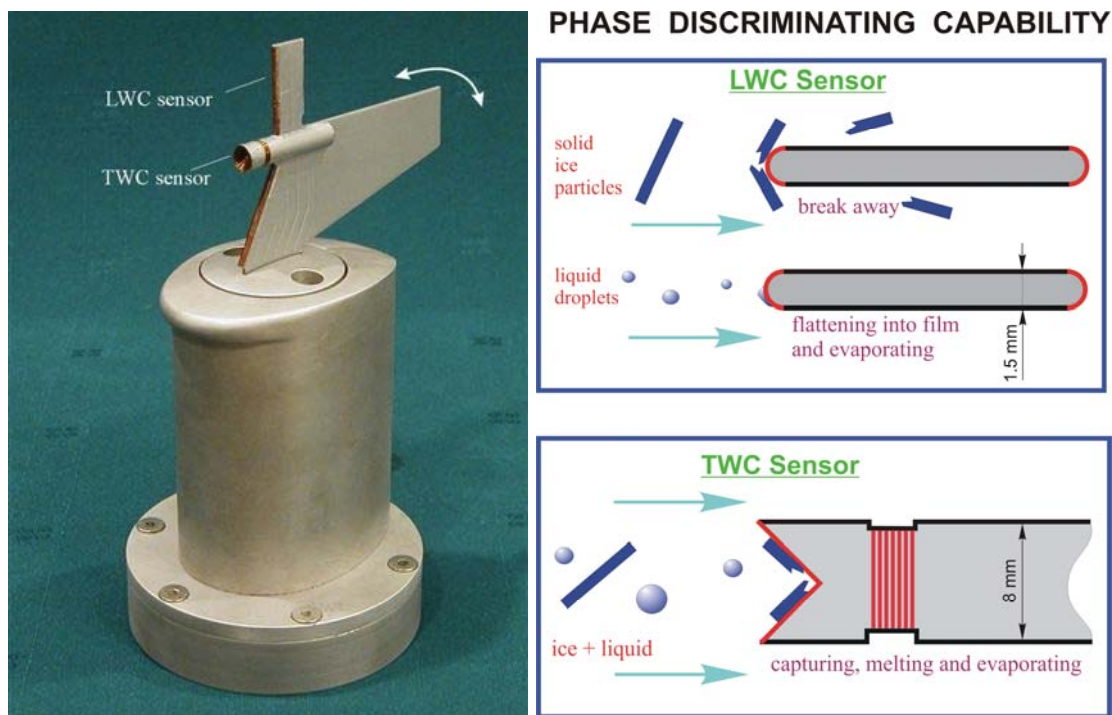


Figure 1. A photo of the Nevzorov liquid water and total water content sensors and a schematic of how the probe works (from Korolev et al., 1998). The TWC Sensor cone is 8 mm wide and 3.5 mm deep.

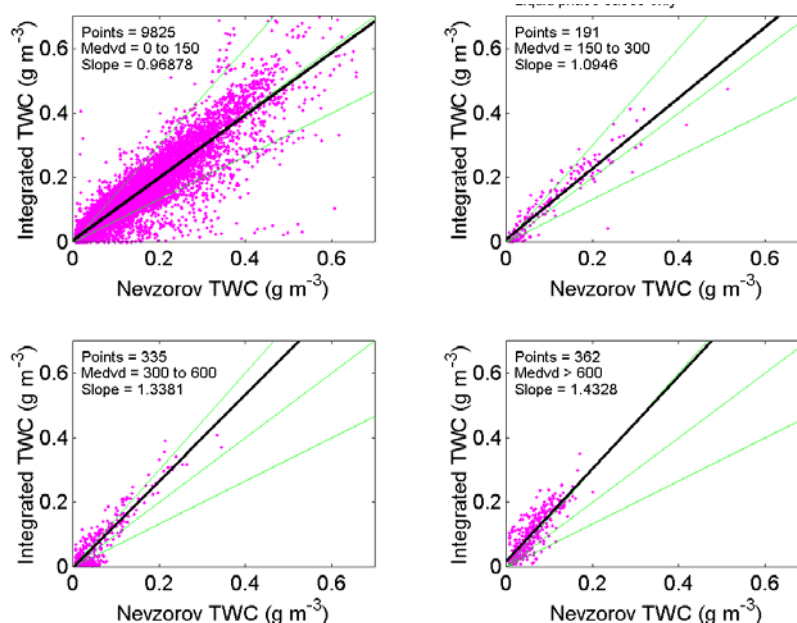


Figure 2. A comparison of the integrated LWC, using PMS FSSP and OAP probes, with the Nevzorov TWC as a function of MVD (Medvd) calculated using the spectra. See Cober and Isaac (2006) for a description of the data set.





Figure 3. Photographs of the Nevzorov Probe mount and camera as used on the NRC-Convair-580 including from left to right: a) photo of roof of aircraft looking forward, b) camera mount inside cabin, and probe mount before installation on aircraft. The distance from the aircraft skin to the probe sensor is 38.4 cm, and the distance from the skin to the light is 49.5 cm.

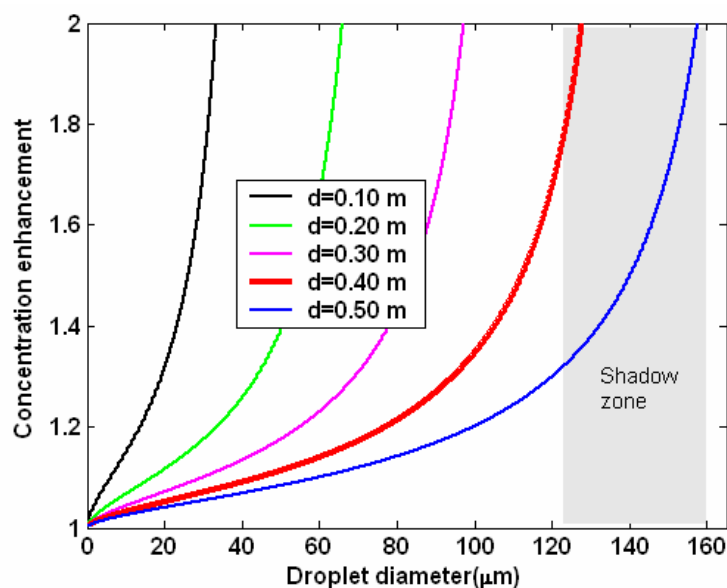


Figure 4. The concentration enhancement calculated based on the *King* (1984) droplet trajectory and air flow model plotted as a function of distance from the fuselage surface of the Convair-580 aircraft and the droplet diameter. The airspeed was assumed to be  $100 \text{ ms}^{-1}$ . The Nevzorov probe was placed roughly at 0.38 m from the Convair's skin. Particles greater than about  $120 \text{ }\mu\text{m}$  will be in a shadow zone (shaded area). For the Convair, the shadow zone maximum occurs at a droplet diameter  $160 \text{ }\mu\text{m}$ . Twohy and Rogers (1993), using more sophisticated models, have shown that much larger particles, with greater inertia, will cross the streamlines and not be shadowed.

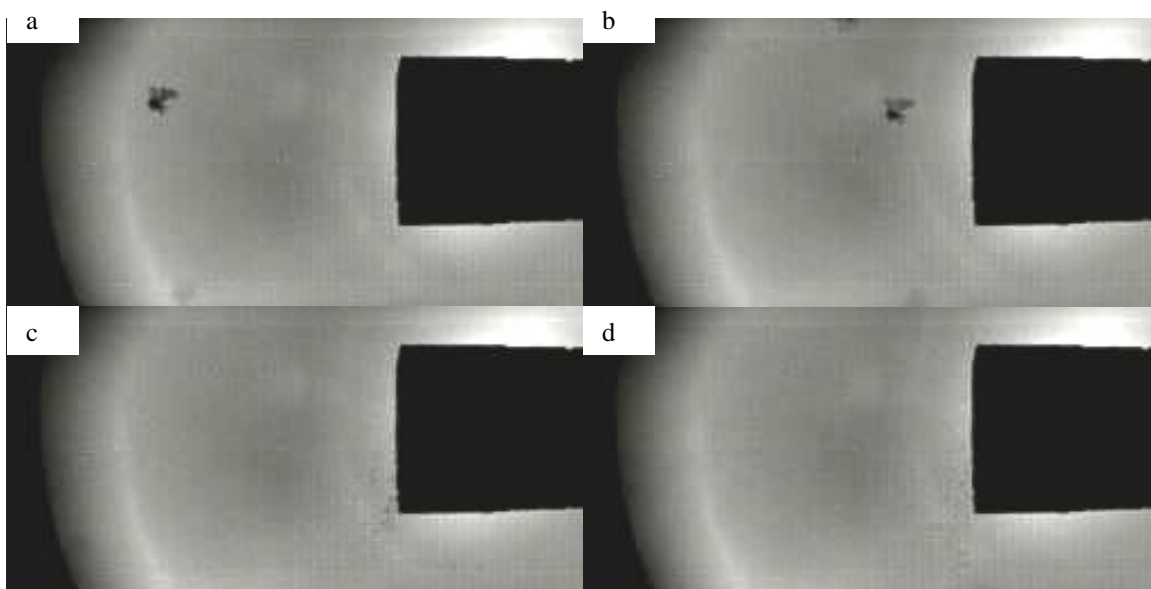


Figure 5. A sequence (a to d) of pictures from Run 6 on 18 December. Shows an ice particle (1mm in size) impacting with the cone of the TWC sensor and several frames later a large number (100s) of particles are ejected from the cone towards the bottom of the pictures

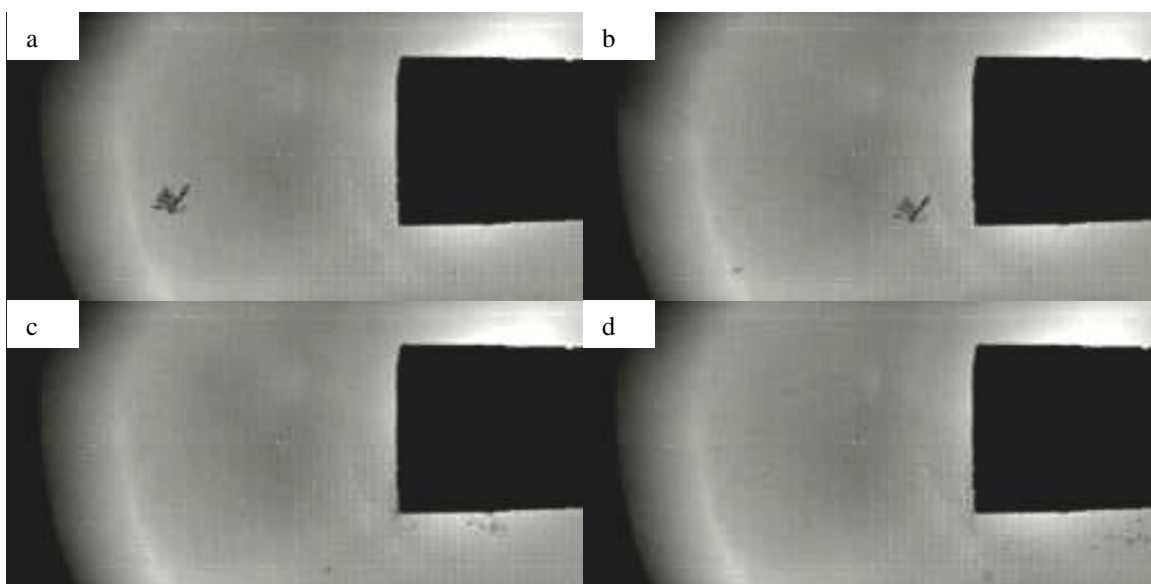


Figure 6. A sequence (a to d) of pictures from Run 6 on 18 December. Shows an ice particle (1.5 mm in size) impacting with the edge of the cone of the TWC sensor and shattering into many pieces.

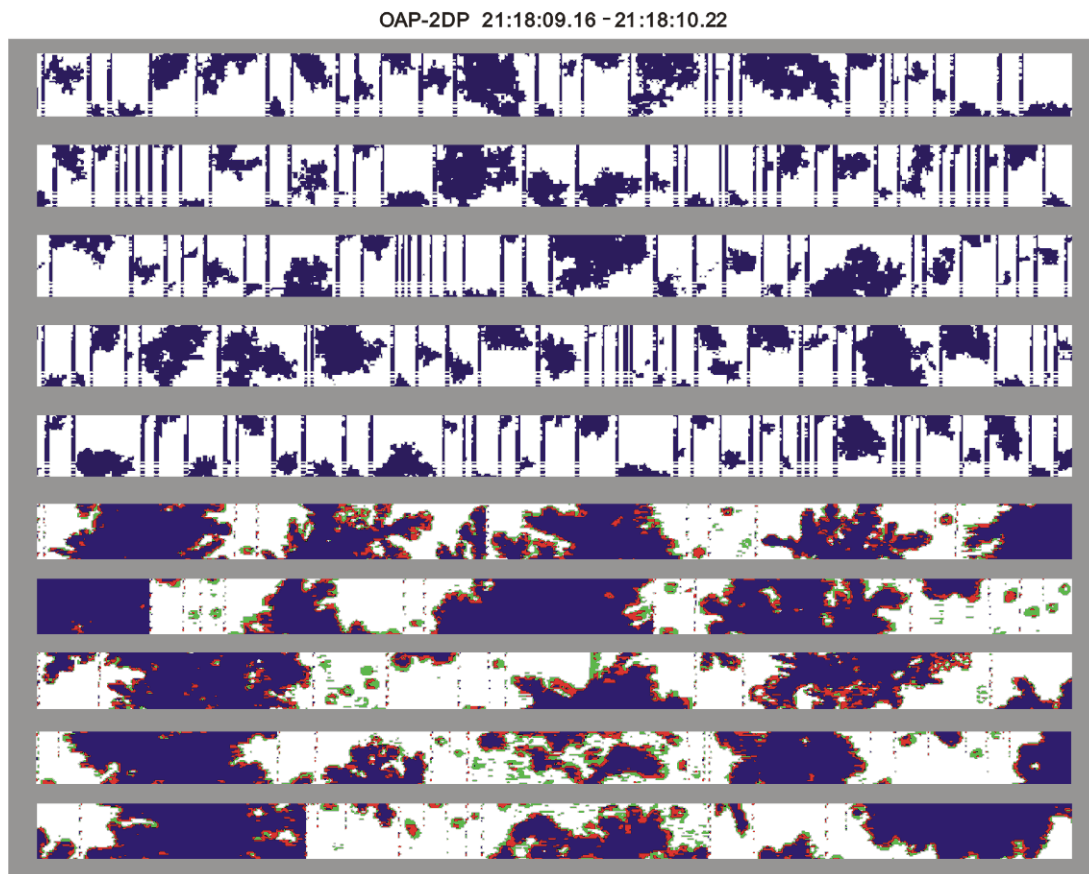


Figure 7. PMS 2DP (top) and 2DC Gray (bottom) images from Run 6 on 18 December. The particles are separated by time bars and the width of each strip is approximately 6.4 mm for the 2DP and 1mm for the 2DG. The images clearly show that large aggregates of dendritic type crystals were being encountered.

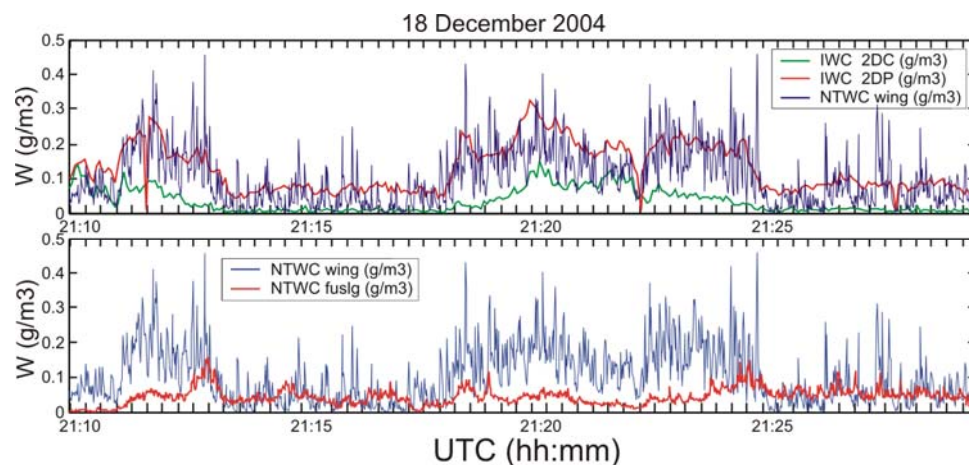


Figure 8. Convair-580 cloud microphysical data near the time of Run 6 (21:18 UTC) on 18 December. The top panel shows a time history of the integrated ice water content (IWC) from the PMS 2DC and 2DP probes and the Nevzorov wing mounted TWC. The bottom panel shows the Nevzorov wing mounted and fuselage mounted Nevzorov TWC.

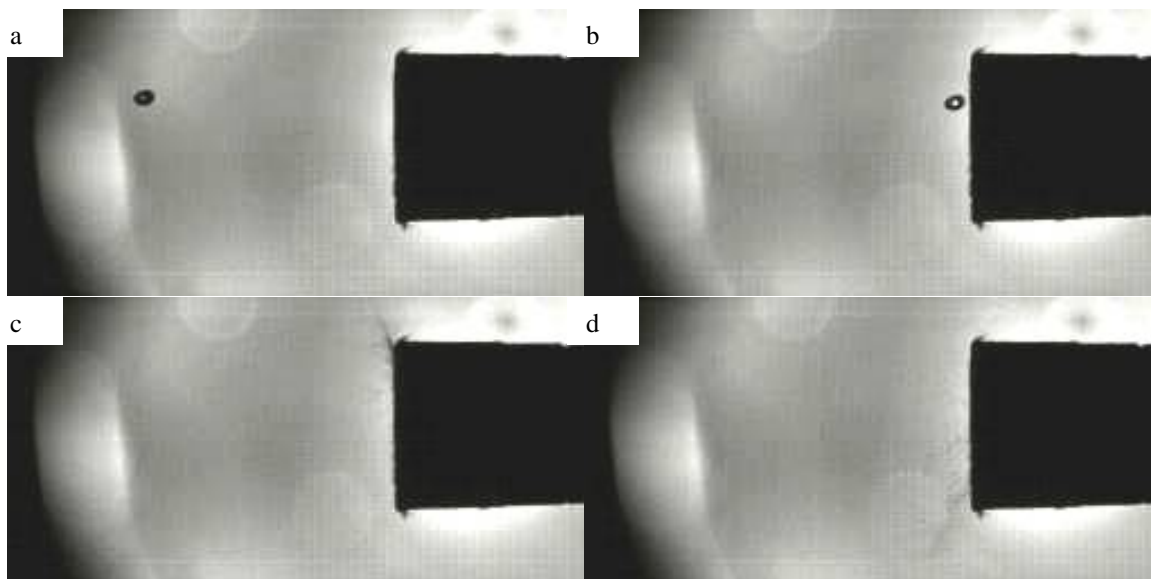


Figure 9. A sequence (a to d) of pictures from Run 8 on 19 December. Shows a water drop ( $750\ \mu\text{m}$  in size) impacting with the cone of the TWC sensor and splashing droplets both up, down and forward of the sensor.

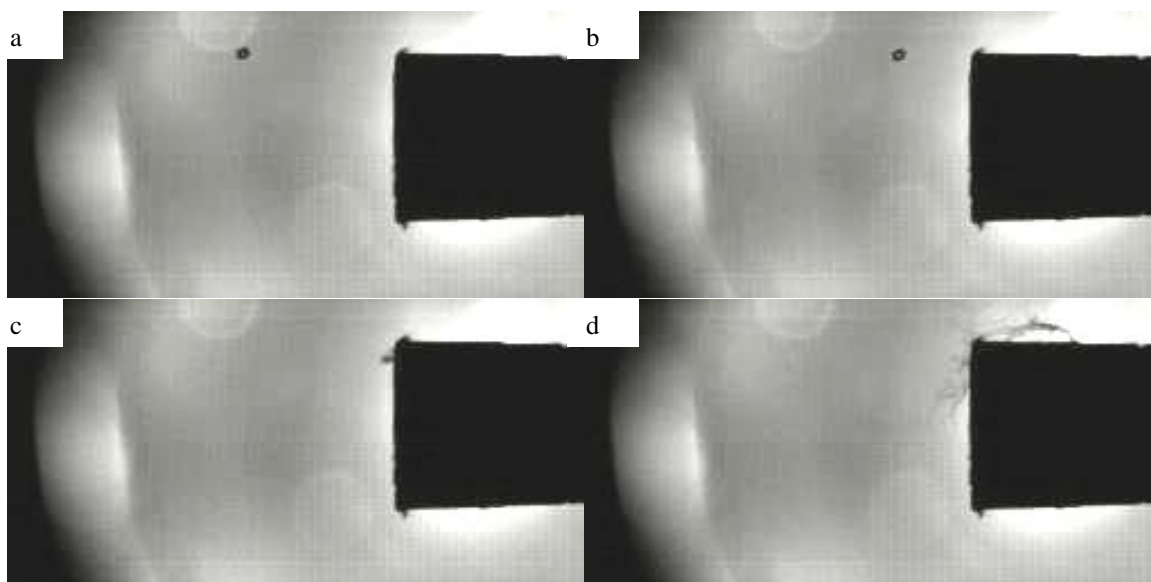


Figure 10. A sequence (a to d) of pictures from Run 8 on 19 December. Shows a water drop ( $500\ \mu\text{m}$  in size) impacting with the edge of the cone of the TWC sensor and producing a wide splash pattern on top and outward from the sensor.

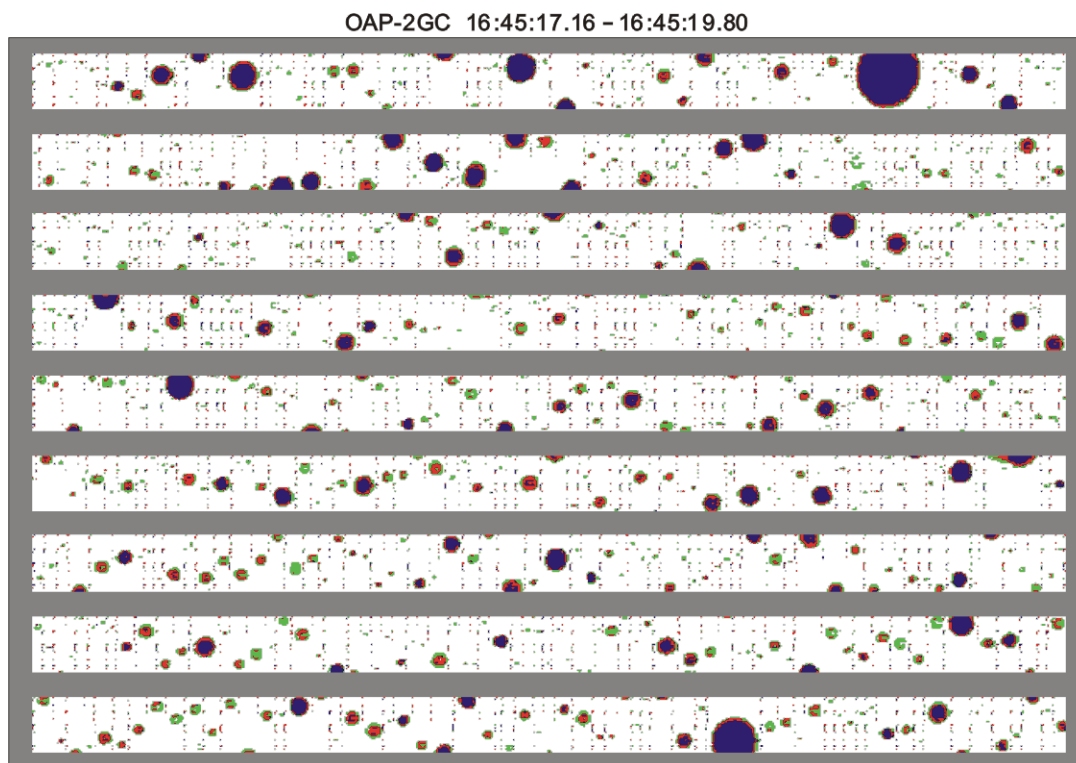


Figure 11. PMS 2DC Gray images from Run 8 on 19 December. The particles are separated by time bars and the width of each strip is approximately 1mm. The images clearly show that large drops were being encountered with maximum sizes just less than 1 mm,

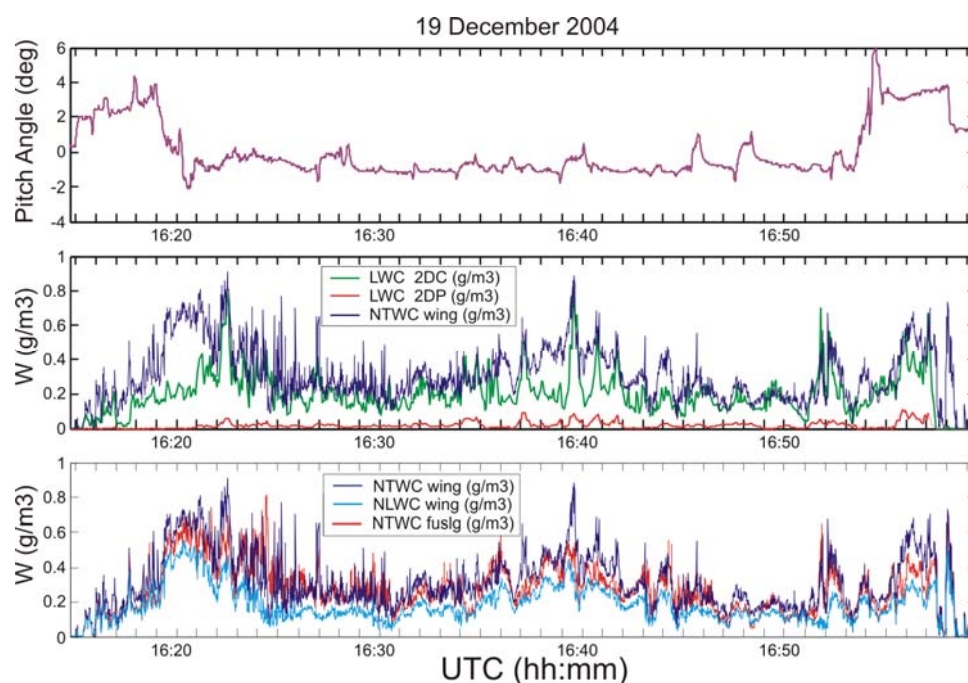


Figure 12. Convair-580 cloud microphysical data near the time of Run 8 (16:45 UTC) on 19 December. The top panel shows the aircraft pitch angle. The middle panel shows a time history of the integrated liquid water content from the PMS 2DC and 2DP probes and the Nevzorov wing mounted TWC. The bottom panel shows the Nevzorov wing mounted and fuselage mounted Nevzorov TWC.